Performance of Decision-Directed Channel Estimation Using Low-Rate Turbo Codes for DFT-Precoded OFDMA

Keita Miwa†, Nobuhiko Miki††, Teruo Kawamura†††, and Mamoru Sawahashi†

† Department of Information Network Engineering, Tokyo City University
†† Research Laboratories, NTT DOCOMO, INC.
††† Radio Access Network Development Department, NTT DOCOMO, INC.

Abstract
A low-rate turbo code can reduce the required average received signal-to-noise power ratio (SNR) that satisfies the target block error rate (BLER) due to its high coding gain. When a low-rate turbo code is used however, channel estimation (CE) error becomes a bottleneck in bringing out the potential coding gain. Therefore, this paper presents the average BLER performance using decision-directed channel estimation (DDCE) for a low-rate turbo code in uplink Discrete Fourier transform (DFT)-precoded orthogonal frequency division multiple access (OFDMA). In the proposed DDCE, we employ soft-decision symbol estimation based on the log-likelihood ratio (LLR) of an extrinsic probability at the Max-Log-MAP (maximum *a posteriori* probability) decoder output in addition to reference signals (RSs). The DDCE works synergistically with the low-rate turbo code, since the extrinsic LLR at the Max-Log-MAP decoder becomes more reliable due to the increasing coding gain. Computer simulation results show that when the turbo code with R = 1/15 (1/9) and the constraint length of K = 4 bits is used, the required average received SNR at the average BLER of 10^{-2} using the DDCE is decreased by approximately 0.6 (0.4) dB compared to that for the RS based CE. As a result, the required average received SNR using the DDCE for R = 1/15 and 1/9 is decreased by approximately 7.0 and 5.0 dB, respectively, compared to that for R = 1/3.

I. Introduction

Establishing wide area coverage is one of the most important requirements in a cellular system. The single-carrier frequency division multiple access (SC-FDMA) scheme achieves a lower peak-to-average power ratio (PAPR) feature than multicarrier based radio access including orthogonal frequency division multiplexing (OFDM). Hence, SC-FDMA was adopted in the Release 8 Long-Term Evolution (LTE) (Rel. 8 hereafter) uplink for its prioritization of wide area coverage provisioning due to a reduction in the transmission back-off in the transmitter power amplifier [1]. Discrete Fourier transform (DFT)-precoded OFDMA (also called DFT-spread OFDMA) was adopted to generate SC-FDMA signals in the frequency domain [2],[3] to achieve high commonality with OFDM in the Rel. 8 LTE downlink and affinity to frequency domain equalizers (FDEs) [4]-[6].

In the LTE, one-cell frequency reuse is adopted to achieve higher capacity than that for High-Speed Downlink Packet Access (HSDPA) / High-Speed Uplink Packet Access (HSUPA). Hence, a set of user equipment (UE) suffers from high-level interference from the surrounding cells. The received signal-to-interference plus noise power ratio (SINR) during a transmission time unit called the transmission time interval (TTI) becomes lower than 0 dB. Thus, an efficient channel coding scheme with high coding gain is essential. As a result, the turbo code [7] is adopted for a shared channel carrying user traffic data due to a high coding gain and commonality with HSDPA/HSUPA and Wideband Code Division Multiple Access (WCDMA). In the Rel. 8 LTE, the minimum coding rate of the turbo code is R = 1/3 [8]. A coding rate higher than R = 1/3 is generated by puncturing parity bits periodically for the mother code with R = 1/3. A coding rate lower than R = 1/3 is generated by a combination of an R = 1/3-turbo code and repetition code. However, a coding rate lower than R = 1/3 for the turbo code is effective in decreasing the required receive signal-to-noise power ratio (SNR) that satisfies the target block error rate (BLER) [9]-[11]. In particular, the maximum transmission power of a UE is much lower than that for a base station (BS), which is referred to as an eNode B. Hence, support of the operation region for a received SNR lower than 0 dB leads to the extension of the coverage area in power-limited environments. In interference-limited environments, the support brings about an increase in the cell throughput, i.e., capacity by applying other-cell interference cancellation at a BS. Note that in LTE and LTE-Advanced, orthogonality for intra-cell interference is already achieved. Under such very low SNR conditions than 0 dB, nevertheless, the increasing channel estimation (CE) error in coherent detection using a reference signal (RS) becomes a bottleneck for reducing the required received SNR to achieve the target BLER. That is, the increasing CE error may offset the additional coding gain by lowering the coding rate.

In the paper, we present the average BLER performance using decision-directed channel estimation (DDCE) for a low-rate turbo code in the uplink DFT-precoded OFDMA. We employ a soft-decision symbol estimate based on the log-likelihood ratio (LLR) of an extrinsic probability at the Max-Log-MAP (maximum *a posteriori* probability) decoder [12] output in addition to RS symbols for DDCE. It is anticipated that the DDCE works synergistically with a low-rate turbo code, since the extrinsic LLR at the Max-Log-MAP decoder becomes more reliable due to the increasing coding gain. Hence, after reducing the CE error by applying DDCE, we investigate the achievable gain for a low-rate turbo code in terms of the reduction in the required average received SNR. The rest of the paper is organized as follows. First, Section II describes the feature of low-rate turbo codes used in the paper. Section III explains the operations of a receiver including DDCE. Then, the computer simulation configuration is given in Section IV. Finally, Section V presents the simulation results followed by the conclusion.

978-1-4673-0990-5/12/$31.00 ©2012 IEEE

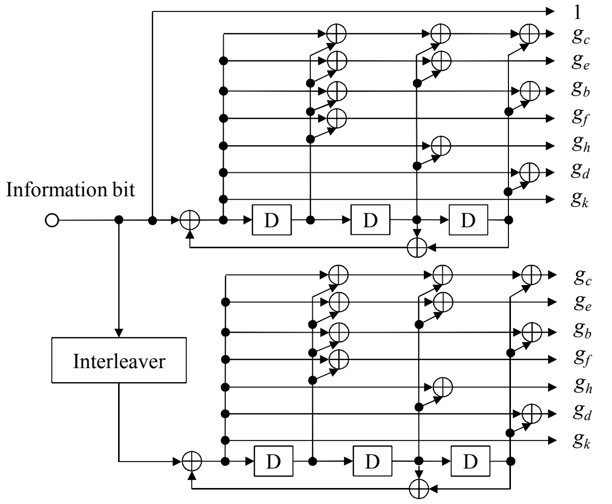

Figure 1. Structure of low-rate turbo encoder.

II. TRANSMITTED SIGNAL REPRESENTATION

The frame structure assumed in the paper is based on that for Rel. 8 LTE [1]. One subframe with a length of 1-msec comprises 14 fast Fourier transform (FFT) blocks, which correspond to the SC-FDMA symbols. Moreover, 1 FFT block contains a 66.7-μsec effective data block and 4.7-μsec cyclic prefix (CP). The corresponding subcarrier spacing becomes 15 kHz. The RS symbols used for channel estimation of coherent detection are multiplexed with the data symbols using time division multiplexing (TDM) into the 4th and 11th FFT blocks. One resource block (RB) comprises 12 subcarriers in the frequency domain and one subframe in the time domain.

The information bit is channel-encoded using a turbo code with the coding rate of R and with the constraint length of K = 4 bits. Fig. 1 shows the structure of a turbo encoder with two constituent codes for K = 4 bits, which we use in the paper [10], [11]. The generator polynomials are given as follows.

- $R = 1/3$: $\boldsymbol{G}_{1/3} = (1, \boldsymbol{g}_b/\boldsymbol{g}_a)$ and $(\boldsymbol{g}_b/\boldsymbol{g}_a)$ where $\boldsymbol{g}_a$ = [1011] and $\boldsymbol{g}_b$ = [1101].
- $R = 1/5$: $\boldsymbol{G}_{1/5} = (1, \boldsymbol{g}_c/\boldsymbol{g}_a, \boldsymbol{g}_b/\boldsymbol{g}_a)$ and $(\boldsymbol{g}_c/\boldsymbol{g}_a, \boldsymbol{g}_b/\boldsymbol{g}_a)$ where $\boldsymbol{g}_c$ = [1111], and $\boldsymbol{g}_a$ and $\boldsymbol{g}_b$ are identical to those for $R = 1/3$.
- $R = 1/7$: $\boldsymbol{G}_{1/7} = (1, \boldsymbol{g}_c/\boldsymbol{g}_a, \boldsymbol{g}_b/\boldsymbol{g}_a, \boldsymbol{g}_d/\boldsymbol{g}_a)$ and $(\boldsymbol{g}_c/\boldsymbol{g}_a, \boldsymbol{g}_b/\boldsymbol{g}_a, \boldsymbol{g}_d/\boldsymbol{g}_a)$ where $\boldsymbol{g}_d$ = [1001], and the other polynomials are identical to those for $R = 1/5$.
- $R = 1/9$: $\boldsymbol{G}_{1/9} = (1, \boldsymbol{g}_c/\boldsymbol{g}_a, \boldsymbol{g}_e/\boldsymbol{g}_a, \boldsymbol{g}_b/\boldsymbol{g}_a, \boldsymbol{g}_d/\boldsymbol{g}_a)$ and $(\boldsymbol{g}_c/\boldsymbol{g}_a, \boldsymbol{g}_e/\boldsymbol{g}_a, \boldsymbol{g}_b/\boldsymbol{g}_a, \boldsymbol{g}_d/\boldsymbol{g}_a)$ where $\boldsymbol{g}_e$ = [1110], and the other polynomials are identical to those for $R = 1/7$.
- $R = 1/11$: $\boldsymbol{G}_{1/11} = (1, \boldsymbol{g}_c/\boldsymbol{g}_a, \boldsymbol{g}_e/\boldsymbol{g}_a, \boldsymbol{g}_b/\boldsymbol{g}_a, \boldsymbol{g}_f/\boldsymbol{g}_a, \boldsymbol{g}_d/\boldsymbol{g}_a)$ and $(\boldsymbol{g}_c/\boldsymbol{g}_a, \boldsymbol{g}_e/\boldsymbol{g}_a, \boldsymbol{g}_b/\boldsymbol{g}_a, \boldsymbol{g}_f/\boldsymbol{g}_a, \boldsymbol{g}_d/\boldsymbol{g}_a)$ where $\boldsymbol{g}_f$ = [1100], and the other polynomials are identical to those for $R = 1/9$.
- $R = 1/13$: $\boldsymbol{G}_{1/13} = (1, \boldsymbol{g}_c/\boldsymbol{g}_a, \boldsymbol{g}_e/\boldsymbol{g}_a, \boldsymbol{g}_b/\boldsymbol{g}_a, \boldsymbol{g}_f/\boldsymbol{g}_a, \boldsymbol{g}_h/\boldsymbol{g}_a, \boldsymbol{g}_d/\boldsymbol{g}_a)$ and $(\boldsymbol{g}_c/\boldsymbol{g}_a, \boldsymbol{g}_e/\boldsymbol{g}_a, \boldsymbol{g}_b/\boldsymbol{g}_a, \boldsymbol{g}_f/\boldsymbol{g}_a, \boldsymbol{g}_h/\boldsymbol{g}_a, \boldsymbol{g}_d/\boldsymbol{g}_a)$ where $\boldsymbol{g}_h$ = [1010], and the other polynomials are identical to those for $R = 1/11$.
- $R = 1/15$: $\boldsymbol{G}_{1/15} = (1, \boldsymbol{g}_c/\boldsymbol{g}_a, \boldsymbol{g}_e/\boldsymbol{g}_a, \boldsymbol{g}_b/\boldsymbol{g}_a, \boldsymbol{g}_f/\boldsymbol{g}_a, \boldsymbol{g}_h/\boldsymbol{g}_a, \boldsymbol{g}_d/\boldsymbol{g}_a, \boldsymbol{g}_k/\boldsymbol{g}_a)$ and $(\boldsymbol{g}_c/\boldsymbol{g}_a, \boldsymbol{g}_e/\boldsymbol{g}_a, \boldsymbol{g}_b/\boldsymbol{g}_a, \boldsymbol{g}_f/\boldsymbol{g}_a, \boldsymbol{g}_h/\boldsymbol{g}_a, \boldsymbol{g}_d/\boldsymbol{g}_a, \boldsymbol{g}_k/\boldsymbol{g}_a)$ where $\boldsymbol{g}_k$ = [1000], and other polynomials are identical to those for $R = 1/13$.

A random interleaver is employed as a turbo interleaver. The bit-interleaver within the duration of one subframe is applied as a channel interleaver. However, the randomization effect from burst error by the channel interleaver is slight due to a short subframe length. The coded bit sequence is QPSK-modulated. Let N_{sbf} and M be the number of FFT blocks (SC-FDMA symbols) carrying user data within one subframe and the number of data-modulated symbols within one FFT block, respectively. Moreover, let $x_k^{(i)}$ be a data-modulated symbol of the i-th FFT block ($0 \le i \le 13$) for the k-th data-modulated symbol ($k = 0,\ldots, M$-1), where M denotes the DFT size, which corresponds to the number of subcarriers within the UE transmission bandwidth, B_{Tx}. In the evaluations in Section IV, we set M = 144, i.e., B_{Tx} = 12 RBs except for Fig. 6. In Fig. 6, the value of M is parameterized. Note that the modulation phase is known at the receiver for the RS symbols for i = 3 and 10. The i-th FFT block is expressed as $\mathbf{x}^{(i)} = \left[x_0^{(i)}, x_1^{(i)}, \cdots, x_{M-1}^{(i)}\right]^T$ in vector notation. The data-modulated symbol sequence is converted by M-point DFT $\mathbf{F}_M$ into a frequency domain signal with M components (subcarriers), $\mathbf{s}^{(i)} = \mathbf{F}_M \mathbf{x}^{(i)}$. In the subcarrier mapping part, the symbol vector, $\mathbf{s}^{(i)}$, is mapped into the assigned transmission bandwidth assuming a localized FDMA signal. The operation of the subcarrier mapping is expressed as an N_{FFT} x M matrix, $\mathbf{Q}_{N_{FFT}\times M}$ $(N_{FFT} \ge M)$, where N_{FFT} denotes the number of points for the following inverse FFT (IFFT). In the paper, we set N_{FFT} = 1024. Matrix $\mathbf{Q}_{N_{FFT}\times M}$ is given as $\mathbf{Q}_{N_{FFT}\times M} = \left(\mathbf{0}_{q\times M} \quad \mathbf{I}_M \quad \mathbf{0}_{(N_{FFT}-q-M)\times M}\right)^T$, where q ($q \in \{0,1,\ldots(N_{FFT} - M - 1)\}$) represents the subcarrier position in which the 0-th subcarrier of the M-subcarrier signal is assigned and $\mathbf{I}_M$ denotes the M x M unit matrix. After padding (N_{FFT} - M) zeros, IFFT converts the frequency-domain signal into a time-domain signal as $\mathbf{y}^{(i)} = \mathbf{F}_{N_{FFT}}^{-1} \mathbf{Q}_{N_{FFT} x M} \mathbf{s}^{(i)}$. Here $\mathbf{F}_{N_{FFT}}^{-1}$ indicates the IFFT matrix. Finally, a CP is appended to each FFT block to avoid inter-block interference.

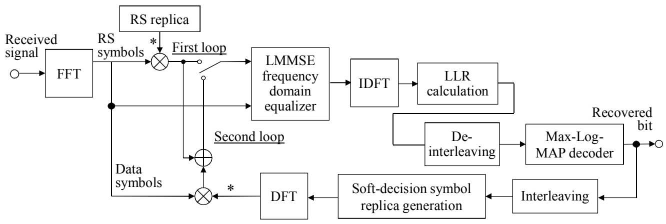

Figure 2. Block diagram of receiver using DDCE.

III. RECEIVER STRUCTURE WITH DDCE

Fig. 2 shows the overall receiver configuration including the DDCE. At the receiver, two-branch antenna diversity reception is assumed. We assume ideal FFT timing detection. After removing the CP, the time domain sample sequence is converted into a frequency domain sample sequence using the FFT. Then, we obtain the desired signals with M subcarriers by removing (N_{FFT} -M) subcarrier components. Let $H_q(u)$ be the channel response between the transmitter antenna and the q-th receiver antenna, and q (q = 0, 1) at each subframe. To reduce the influence of the noise component, we compute a channel estimate at the u-th subcarrier (u = 0, 1, …, M-1),

$\widehat{H}_q(u)$, by coherent averaging over $2F_{avg}+1$ subcarriers with the subcarrier of interest as the center as

$$\widehat{H}_q(u)=\sum_{f=-F_{avg}}^{F_{avg}}\alpha_f H_q(u+f). \quad (1)$$

In (1), coherent summation using weighting factor α_f ($\sum_{f=-F_{avg}}^{F_{avg}}\alpha_f=1$) is employed. In the evaluation, we set $\lfloor\alpha_0,\alpha_{+1/-1},\alpha_{+2/-2},\alpha_{+3/-3},\alpha_{+4/-4}\rfloor=[0.2,0.16,0.12,0.08,0.04]$ for F_{avg} = 4. The computed $\widehat{H}_q(u)$ is further coherently averaged to $\overline{H}_q(u)$ over two RS symbols within the duration of a subframe using the channel estimate at each subcarrier after frequency and time domain averaging. The linear minimum mean square error (LMMSE) weight at the u-th subcarrier at the h-th receiver branch, $W_q(u)$, is computed as [4]

$$W_q(u)=\overline{H}_q^{\,*}(u)\Big/\left(\sum_{q'=0}^{1}\left|\overline{H}_{q'}(u)\right|^2+\sigma\right). \quad (2)$$

In (2), we assume ideal estimation of the noise component, σ, in the denominator of the LMMSE weight. Maximal ratio combing (MRC) is employed for receiver antenna combining. We compute the squared Euclidian distance between the received symbol after equalization and the symbol replica candidate using the estimated channel impulse response for both bits "0" and "1." We compute the LLR of *a posteriori* probability (APP) using the minimum squared Euclidian distance for bits "0" and "1" [12]. Finally, the LLR is soft-decision turbo decoded using Max-Log-MAP decoding [13] with eight iterations to recover the transmitted binary data.

In the DDCE, the LLR is computed for coded bits after turbo coding at the Max-Log-MAP decoder output. Let $\lambda(v_{n,p})$ be the LLR for extrinsic information of the p-th bit of the n-th data symbol at the last iteration, i.e., $\lambda(v_{n,p})=\log\{P(v_{n,p}=1)/P(v_{n,p}=0)\}$. Then, using the extrinsic LLR, the soft-symbol estimate for the n-th data symbol is computed as [14]

$$\hat{x}_n=\tanh\left(\frac{\lambda(v_{n,p_I})}{2}\right)+j\tanh\left(\frac{\lambda(v_{n,p_Q})}{2}\right), \quad (3)$$

where p_I and p_Q are the in-phase bit and quadrature bit associated with the n-th data symbol. Then, by multiplying $\hat{x}_n$ and its complex conjugate, the frequency domain channel response at the i-th FFT block (i = n mode N_{FFT}) at the q-th receiver branch, $H_q^{(i)}(u)$, is computed. The channel response at the u-th subcarrier is coherently averaged over 14 FFT blocks including the two RS symbols as $\widehat{H}_q(u)=\sum_{i=0}^{13}\widehat{H}_q^{(i)}(u)$. Similar to the initial channel estimation using only the RS symbols, the noise suppression filter in the frequency domain in (1) is employed. The squared Euclidian distance between the received symbol after receiver diversity combining and the symbol replica candidate for both bits "0" and "1" are fed into the Max-Log-MAP decoder. Finally, the output LLR of the Max-Log-MAP decoder is hard-decided to recover the transmitted bit sequence.

IV. COMPUTER SIMULATION RESULTS

Table I gives the simulation parameters assumed in the paper. The nine-path Extended Typical Urban (ETU) channel model with the root mean square (r.m.s.) delay spread of 0.99 μsec [15] is assumed for the multipath delay profile model. Moreover, the Extended Vehicular-A (EVA) channel model with the r.m.s. delay spread of 0.36 μsec [15] is assessed as a reference. The fading maximum Doppler frequency is set to f_D = 5.55 Hz, which corresponds to the moving speed of 3 km/h at the carrier frequency of 2 GHz.

TABLE I. MAJOR RADIO PARAMETERS

Transmission bandwidth		10 MHz
Number of FFT samples		1024
Subcarrier spacing		15 kHz
Subframe length		1 msec (14 FFT blocks)
Symbol duration	Effective symbol duration	66.7 μsec
	Cyclic prefix	4.7 μsec
Data modulation		QPSK
Channel coding / Decoding		Turbo code (R = 1/15-1/3, K = 4) / Max-Log-MAP decoding (8 iterations)
Number of receiver antennas		2
Channel model		Extended TU (ETU) channel model Extended Veh.-A (EVA) channel model
Maximum Doppler frequency, f_D		5.55Hz

First, Figs. 3(a) and 3(b) show the average BLER performance of the DDCE using R = 1/9 and 1/15 as a function of the average received SNR per receiver antenna for DFT-precoded OFDMA. We assume the ETU channel model. We also plot the average BLER performance for OFDMA assuming the same number of subcarriers, RS structure, and CE method at each subcarrier as those for DFT-precoded OFDMA. In addition to the performance of the DDCE using soft-symbol estimation, the performance of that using hard-symbol estimation is plotted, in which the extrinsic LLR at the Max-Log-MAP decoder output is hard-decided. Frist, we focus on the effect of the DDCE in DFT-precoded OFDMA. From Fig. 3(a), the required average received SNR at the average BLER of 10^{-2} using the DDCE with soft- or hard-symbol estimation is decreased by approximately 0.4 or 0.2 dB, respectively, compared to that for RS based CE for R = 1/9. The resultant loss in the required average received SNR of the DDCE using soft-symbol estimation from ideal CE is approximately 1.4 dB. From Fig. 3(b), by decreasing R from 1/9 to 1/15, the required average received SNR region becomes lower by approximately 2.2 dB to satisfy the same average BLER. Hence, the loss in the required average received SNR of the RS based CE from ideal CE increases to approximately 2.2 dB. However, the loss of the DDCE using soft-symbol estimation from ideal CE for R = 1/15 is reduced almost to the same level as that for R = 1/9, i.e., such as approximately 1.6 dB. Hence, we see that the DDCE with soft-symbol estimation is effective in suppressing the loss in the required average received SNR due to the CE error for a low-rate coding rate. Next, we focus on the performance difference between DFT-precoded OFDMA and OFDMA with a low-rate turbo code. From Figs. 3(a) and 3(b), the average BLER performance levels for DFT-precoded OFDMA are almost identical to those for OFDMA with ideal CE and RS based CE. Hence, we see that the difference in the influence of the CE error between on the LMMSE weight generation in the FDE for DFT-precoded OFDMA and that on coherent detection for OFDMA is small. Meanwhile, using the DDCE, the average BLER performance for DFT-precoded OFDMA is degraded by approximately 0.5 and 0.3 dB compared to that for OFDMA with R = 1/9 and 1/15, respectively. It is considered that the loss is due to the influence of the decoding errors in the Max-Log-MAP decoder. In the following evaluations, we use the DDCE with soft-symbol estimation.

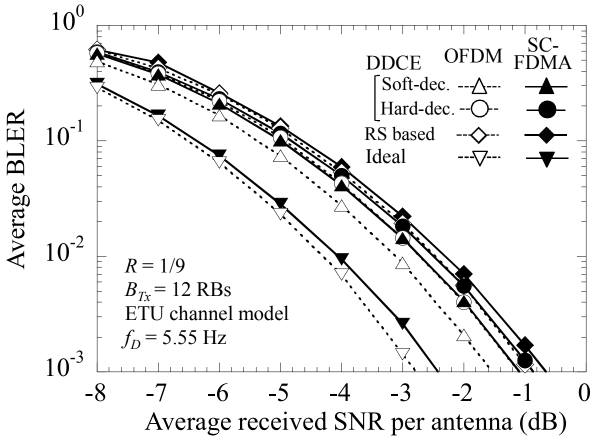

(a) R = 1/9

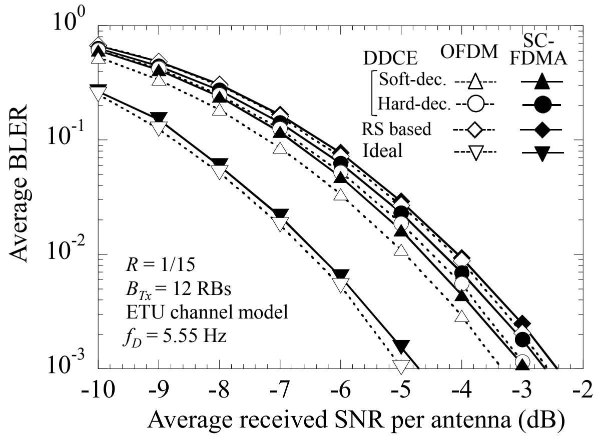

(b) R = 1/15

Figure 3. Average BLER performance as a function of average received SNR for ETU channel model.

Fig. 4 shows the average BLER performance of the DDCE as a function of the received SNR with the coding rate, R, as a parameter, for DFT-precoded OFDMA in the ETU channel model. Fig. 4 shows that according to the decrease in the R value, the BLER improves due to the increasing channel coding gain with both the RS based CE and DDCE. However, we clearly see that the improvement in the average BLER performance is reduced according to the decrease in the R value for the RS based CE. This suggests that the increased CE error in the lower received SNR region hinders the increased coding gain from the low-rate turbo code. Meanwhile, we recognize that there is a distinct gain from the low-rate turbo code using the DDCE with soft-symbol estimation under very low received SNR conditions. More specifically, when R = 1/15 (1/11), the required average received SNR at the average BLER of 10^{-2} using the DDCE is decreased by approximately 0.6 (0.5) dB compared to that for the RS based CE. Then, when the DDCE with soft-symbol estimation is employed, the required average received SNR for R = 1/15 and 1/11 is decreased by approximately 7.0 and 6.0 dB compared to that for R = 1/3. As a result, the average BLER of 10^{-2} is achieved at the average received SNR of approximately -4.6 dB using the DDCE associated with the R = 1/15 turbo code. Hence, we see that the DDCE is very effective in bringing out the potential gain from a low-rate turbo code in very low received SNR environments. Furthermore, a turbo code with R = 1/9 deceases the required average received SNR at the average BLER of 10^{-2} by approximately 5.0 dB compared to that for R = 1/3. When a combination of an R = 1/3-turbo code and 3-symbol repetition code is used, which yields the overall coding rate of R = 1/9, the gain in the average received SNR from R = 1/3 is 4.77 dB at maximum. Hence, we see that the low-rate turbo code using R = 1/9 is effective in decreasing the required average received SNR compared to additional usage of repetition coding.

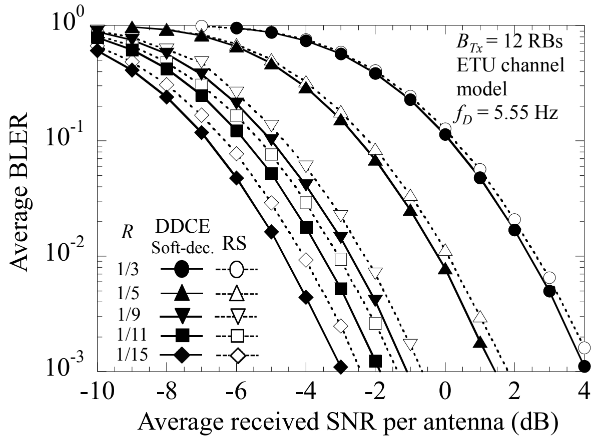

Figure 4. Average BLER performance as a function of average received SNR with R as a parameter for ETU channel model.

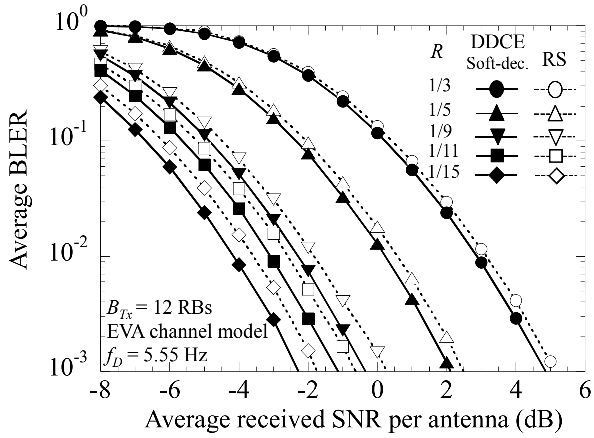

Figure 5. Average BLER performance as a function of average received SNR with R as a parameter for EVA channel model.

Fig. 5 shows the average BLER performance using the

DDCE in the EVA channel model. The other conditions are the same as those in Fig. 4. Compared to the performance in Fig. 4, the BLER performance in the EVA channel model becomes worse due to the decreasing frequency diversity effect caused by the smaller delay spread value. However, the same tendency is observed as those in the ETU channel model. For R = 1/15 (1/11), the required average received SNR at the average BLER of 10^{-2} using the DDCE is decreased by approximately 0.6 (0.5) dB compared to that for the RS based CE. Then, when the DDCE with the soft-symbol estimate is employed, the required average received SNR for R = 1/15 and 1/11 is decreased by approximately 7.0 and 6.0 dB compared to that for R = 1/3. As a result, the average BLER of 10^{-2} is achieved at the average received SNR of approximately -4.2 dB using the DDCE associated with the R = 1/15 turbo code.

Finally, Fig. 6 shows the required average received SNR that satisfies the average BLER of 10^{-2} of the DDCE as a function of the UE transmission in the ETU channel model. The channel coding rate, R, is parameterized. From the figure, the required average received SNR at the average BLER of 10^{-2} is decreased according to the increase in B_{Tx} due to the increasing frequency diversity effect. Moreover, we confirm that the relative gain in decreasing the required average received SNR by reducing the R value is almost identical regardless of B_{Tx}. In summary, the DDCE using the soft-symbol estimate is beneficial in achieving a high coding gain from a low-rate turbo code in the very low SNR operational region.

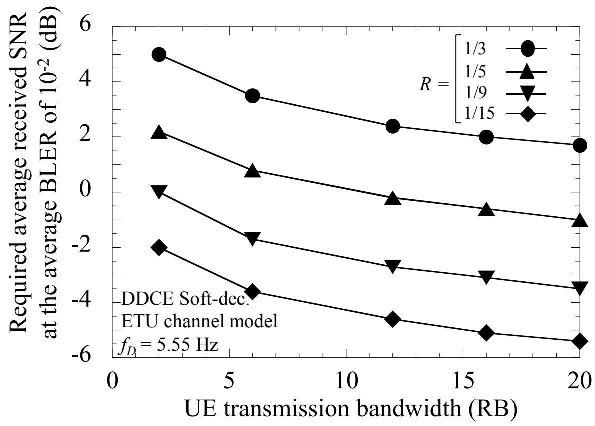

Figure 6. Required average received SNR satisfying the average BLER of 10^{-2} of the DDCE as a function of the UE transmission for ETU channel model.

V. CONCLUSION

This paper presented the average BLER performance using the DDCE for a low-rate turbo code in the uplink DFT-precoded OFDMA. In the proposed DDCE, we employ soft-decision symbol estimation based on the LLR of an extrinsic probability at the Max-Log-MAP decoder output in addition to the RSs. The DDCE works synergistically with a low-rate turbo code, since the extrinsic LLR at the Max-Log-MAP decoder becomes more reliable due to the increasing coding gain. Computer simulation results showed when a low-rate turbo code with R = 1/9 and 1/15 is employed, the average BLER performance for DFT-precoded OFDMA is degraded slightly compared to that for OFDMA with DDCE, while an almost identical average BLER performance level is achieved with RS based CE. We showed when a turbo code with R = 1/15 (1/9) and K = 4 bits are used, the required average received SNR at the average BLER of 10^{-2} using the DDCE is decreased by approximately 0.6 (0.4) dB compared to that for the RS based CE. As a result, the required average received SNRs using the DDCE for R = 1/15 and 1/9 are decreased by approximately 7.0 and 5.0 dB compared to that for R = 1/3, and the average BLER of 10^{-2} is achieved at the average received SNR of approximately -4.6 dB using the DDCE associated with the R = 1/15 turbo code. In conclusion, we confirmed that the DDCE brings out a potentially high coding gain from a low-rate turbo code under very low received SNR conditions.

REFERENCES

[1] 3GPP TS36.211 (V8.9.0), "E-UTRA; Physical channels and modulation," Dec. 2009.

[2] D. Galda and H. Rohling, "A low complexity transmitter structure for OFDM-FDMA uplink system," IEEE VTC2002-Spring, vol. 4, May 2002.

[3] R. Dinis, D. Falconer, C. T. Lam, and M. Sabbaghian, "A multiple access scheme for the uplink of broadband wireless access," IEEE Globecom, vol. 6, Dec. 2004.

[4] H. Sari, G. Karam, and I. Jeanclaud, "Frequency-domain equalization of mobile radio and terrestrial broadcast channels," IEEE Global Telecommunications Conference, vol. 1, Nov.–Dec. 1994.

[5] D. Falconer, S. L. Ariyavisitakul, A. Benyamin-Seeyar, and B. Eidson, "Frequency domain equalization for single-carrier broadband wireless systems," IEEE Commun., Mag., vol. 40, Apr. 2002.

[6] F. Adachi, D. Garg, S. Takaoka, and K. Takeda, "Broadband CDMA techniques," IEEE Commun., Mag., vol. 12, pp. 8–18, Apr. 2005.

[7] C. Berrou and A. Glavieux, "Near optimum error correcting coding and decoding: Turbo codes," IEEE Trans. on Commun., vol. 44, pp. 1261 – 1271, Oct. 1996.

[8] 3GPP, TS36.212 (V8.8.0) , "E-UTRA; Multiplexing and channel coding," Dec. 2009.

[9] D. Divsalar and F. Pollara, "Low-rate turbo codes for deep-space communications," Proc. IEEE International Symposium on Information Theory, 1995.

[10] S. Abeta and H. Kobayashi, "Performance of very low rate channel coding in W-CDMA reverse link," Proc. IEEE PIMRC 2002, pp. 961-965, Sept. 2002.

[11] C. F. Leanderson, J. Hokfelt, O. Edfors, and T. Maseng, "On the design of low rate turbo codes," Proc. IEEE VTC'2002-Spring, pp.1200-1204, May 2000.

[12] P. Robertson, E. Villebrun, and P. Hoeher, "A comparison of optimal and sub-optimal MAP decoding algorithms operating in the log domain," Proc. IEEE ICC'95, vol. 2, pp. 1009-1013, June 1995.

[13] A. Stefanov and T. Duman, "Turbo coded modulation for wireless communications with antenna diversity," Proc. IEEE VTC-Fall, pp. 1565-1569, Sept. 1999.

[14] X. Wang and H. V. Poor, "Iterative (turbo) soft interference cancellation and decoding for coded CDMA," IEEE Trans. Commum., vol. 47, no. 7, pp. 1046-1061, July 1999.

[15] 3GPP TS 36.104 (V10.0.0), Sept. 2010.